

## CYCLIC FATIGUE-CRACK GROWTH IN TOUGHENED CERAMICS AND INTERMETALLICS AT AMBIENT TO ELEVATED TEMPERATURES

R. O. Ritchie and K. T. Venkateswara Rao\*

The role of extrinsic crack-tip shielding on toughness and fatigue-crack growth behavior in intermetallics and ceramics is contrasted with intrinsic damage mechanisms, both at ambient and elevated temperatures. Examples are presented from behavior in an *in situ* toughened SiC ceramic and in ductile-phase toughened  $\gamma$ -TiAl intermetallics. In SiC ceramics, marked R-curve toughening is achieved under monotonic loading by grain bridging, which is diminished under cyclic loading through progressive wear at the sliding grain interfaces. As a result, cyclic crack-growth rates are extremely sensitive to  $K_{max}$  and less dependent on  $\Delta K$ , although at elevated temperatures, behavior is influenced by extrinsic and intrinsic effects associated with deformation and damage of grain-boundary amorphous films. In contrast, fatigue-crack growth in TiNb-reinforced  $\gamma$ -TiAl is a function of both intrinsic and extrinsic mechanisms, intermediate to behavior in metals and ceramics, such that propagation rates are sensitive to both  $\Delta K$  and  $K_{max}$ . However, the marked  $K$ -dependence of growth rates in these materials necessitates the use of design and life-prediction procedures based on crack initiation, small crack or threshold philosophies.

### INTRODUCTION

Over the past ten years, there has been an increasing interest in the use of high-strength, brittle materials, such as ceramics, intermetallics and their respective composites, for structural applications. This has been particularly focused at elevated temperature applications, but in the case of ceramics for biomedical implant devices, at lower temperatures too. Examples of such "advanced materials" are the use of silicon nitride ceramics for automobile turbocharger wheels and engine valves and pyrolytic carbon for prosthetic cardiac devices, and the contemplated use of composite ceramics for gas turbine blades. Similarly, intermetallic alloys, such as the  $\gamma$ -based titanium aluminides, have been considered for applications such as automobile engine valves and compressor blades in gas turbines. Whereas these materials offer vastly improved specific strength at high temperatures compared to conventional metallic alloys, they suffer in general from a pronounced lack of damage tolerance in the form of an extreme sensitivity to pre-existing flaws. Moreover, recently it has become apparent that even low ductility materials such as ceramics show a pronounced susceptibility to premature failure under cyclic fatigue loading (e.g., 1).

The majority of intermetallic and ceramic materials must be toughened, either through composite reinforcement or through the development of novel microstructures, to overcome their limitations of low toughness and ductility at ambient temperature (e.g., 2,3). With advanced materials, such toughening invariably is *extrinsic*, i.e., based on the concept of crack-tip shielding

---

\*Materials Sciences Division, Lawrence Berkeley National Laboratory, and Department of Materials Science and Mineral Engineering, University of California at Berkeley, Berkeley, CA 94720-1760, USA

(1,2). This involves mechanisms that act primarily in the crack wake to reduce the *local* driving force actually experienced at the crack tip through closure tractions imposed in the wake. The approach is rather distinct from toughening in metallic materials. Here, the approach generally involves *intrinsic* mechanisms that enhance the inherent microstructural resistance of the material by phenomena that are generally active in the process zone ahead of the crack tip. Thus, fracture may be envisaged as a mutual competition between intrinsic mechanisms ahead of the crack tip, which act to promote cracking, opposed by extrinsic mechanisms in the wake, which act to inhibit it (Fig. 1). Thermomechanical treatments aimed at variations in grain size, precipitate size and distribution in microstructures of metallic materials like steels, aluminum alloys and superalloys are good examples of intrinsic toughening. Extrinsic mechanisms, on the other hand, are associated with the tractions that may be induced by *in situ* phase transformations, interlocking grains, or by crack bridging resulting from the incorporation of fibers, whiskers or ductile reinforcements in the microstructure. Under cyclic loading, shielding can additionally result from wedging mechanisms in the form of crack closure (4,5). A schematic illustration of various extrinsic mechanisms is given in Fig. 2 (1).

Although crack-tip shielding in brittle materials such as ceramics and ceramic-matrix composites is critical in inducing some degree of toughness, such mechanisms can concurrently render these materials to be susceptible to cyclic fatigue failure (e.g., 6-9). In most ceramics and their respective composites, there appears to be no intrinsic mechanism for cyclic crack advance, at least at low homologous temperatures; the advance of the crack tip proceeds by mechanisms identical to those occurring under monotonic loading (i.e., by static fatigue). However, under cyclic loads, a progressive degradation in the toughening (or shielding) mechanisms can occur behind the crack tip which locally elevates the near-tip driving force. It is this cyclic suppression of shielding that is considered to be the principal source for the susceptibility of brittle materials to cyclic fatigue failure. By contrast, the propagation of fatigue cracks in metallic materials is primarily *intrinsic* damage processes occurring *ahead* of the crack tip; this typically involves crack advance by progressive blunting and resharping of the crack tip (10), i.e., along alternating or simultaneous slip planes (11), clearly mechanisms distinct from fracture under monotonic loads. Shielding, in the form of crack closure (wedging) mechanisms, can act in the crack wake. However, since the physical mechanisms of crack advance and crack-tip shielding are quite different in metals and ceramics, the dependencies on the alternating and mean loads, specifically  $\Delta K$  and  $K_{max}$ , the alternating and maximum stress intensities, respectively, are also quite different. A schematic illustration illustrating these differences is shown in Fig. 3. Indeed, in fatigue the two material classes of metals and ceramics represent the extremes of behavior with respect to the role of intrinsic vs. extrinsic effects on fracture and fatigue; crack-growth behavior in intermetallic materials generally lies somewhere in between. In this paper, examples of fracture and fatigue behavior in selected ceramic and intermetallic systems are presented with specific emphasis on the relative role of intrinsic and extrinsic mechanisms influencing crack growth under monotonic and cyclic loading. The influence of temperature on the fracture and fatigue properties and the resultant implications to structural design and life prediction are also discussed.

### CERAMIC MATERIALS

Most ceramics cannot be toughened intrinsically; invariably toughness at ambient temperature is achieved using extrinsic mechanisms (2). Notable among these are transformation toughening in *in situ* phase-transforming ceramics such as partially-stabilized zirconias, fiber bridging in ceramic-matrix composites such as Nicalon-fiber reinforced LAS glasses, ductile-phase toughening in ceramics reinforced with a metallic phase, such as Al-reinforced  $Al_2O_3$ , and most commonly, interlocking grain bridging in monolithic ceramics such as coarse-grained  $Al_2O_3$  and grain-elongated  $Si_3N_4$ . All these materials develop their toughness through a rising resistance curve (or R-curve), where the driving force for crack growth increases with crack extension as the tractions

that are progressively developed in the crack wake locally shield the crack tip. Such wake toughening mechanisms, however, may degrade under cyclic loading, and it is believed that this is the source of cyclic fatigue failure in most ceramics (6-9). Indeed, fatigue crack advance occurs by a mechanism essentially identical to that seen during monotonic loading but, due to the degraded shielding in the crack wake, at significantly reduced driving forces. A good example of such behavior, for an *in situ* toughened SiC ceramic (12,13), is described below.

#### High-Toughness Silicon Carbide

SiC ceramics generally exhibit excellent creep and oxidation resistance, high thermal conductivity and low thermal expansion properties compared to most other ceramic materials at high temperatures (e.g., 14). The widespread use of monolithic SiC has been limited, however, by its low toughness ( $K_{IC} \sim 2\text{-}3 \text{ MPa}\sqrt{\text{m}}$ ) at ambient temperature. Recent developments in hot-pressed SiC using Al, B, and C as sintering additives (referred to as ABC-SiC) have shown that microstructures consisting of elongated SiC platelets, following the  $\beta(3C)$  to  $\alpha(4H)$  phase transformation, exhibit toughnesses approaching nearly  $10 \text{ MPa}\sqrt{\text{m}}$  (12,13), while retaining a high modulus of rupture ( $\sim 660 \text{ MPa}$ ). Such improvements in the room temperature toughness and strength, however, lead to a susceptibility to fatigue failure and can have a detrimental influence on mechanical properties at high temperatures. Results in ABC-SiC and underlying crack-growth mechanisms are discussed below.

**Behavior at ambient temperatures.** Unlike commercial SiC, ABC-SiC displays rising R-curve behavior under monotonic loading, with crack initiation occurring at  $K_i \sim 5.5 \text{ MPa}\sqrt{\text{m}}$  (for small cracks  $\sim 100 \mu\text{m}$  or less,  $K_i$  is reduced to  $\sim 3.5 \text{ MPa}\sqrt{\text{m}}$ ) and the crack-growth resistance increases over several hundred microns of crack extension to a maximum value of  $K_{IC} \sim 9 \text{ MPa}\sqrt{\text{m}}$  (Fig. 4a). This represents more than a threefold improvement in the toughness of commercial SiC (Hexoloy SA), which shows no R-curve and fails catastrophically at  $K_{IC} \sim 2.5 \text{ MPa}\sqrt{\text{m}}$ . Analogous to behavior in  $\text{Si}_3\text{N}_4$ , the marked increase in fracture resistance of ABC-SiC can be ascribed to the heterogeneous, elongated plate-like grain structure. Crack paths and fracture-surfaces show clear evidence of extensive crack deflection along the  $\alpha$ -grain boundaries, which in turn leads to intergranular cracking (Fig. 4c) and frictional grain bridging (13). In contrast, Hexoloy SA exhibits transgranular cleavage cracking with no significant deflection at grain boundaries and hence no grain bridging, consistent with the absence of an R-curve.

Under cyclic loading, crack-growth rates in ABC-SiC are significantly faster than corresponding (static fatigue) growth rates under monotonic loads at equivalent stress-intensity levels; in both cases, growth rates show a marked dependence on the applied  $K$ . Although the underlying mechanism of crack advance in static and cyclic fatigue appears to be identical, the resulting cyclic fatigue fracture surfaces display evidence of profuse damage and debris (Fig. 4d) which is not observed on static fatigue surfaces (Fig. 4c). The debris results from repetitive contact between the crack faces during cyclic loading, and is a characteristic of the cycle-dependent decay in the interlocking grain bridges (e.g., 7,8). Since Hexoloy SA is not toughened extrinsically, it displays no evidence of cyclic crack growth, as represented by the vertical line in Fig. 4b.

At higher (positive) load ratios ( $R = K_{\text{min}}/K_{\text{max}}$ ), fatigue-crack growth rates are faster (at a given  $\Delta K$ ), with the value of the fatigue thresholds ( $\Delta K_{\text{TH}}$ ), below which "long-crack" growth is presumed dormant, being reduced (Fig. 5a). Such load ratio effects, however, can be normalized by characterizing in terms of the maximum stress intensity,  $K_{\text{max}}$  (Fig. 5b), demonstrating that fatigue-crack propagation in ceramics, unlike in metals (15) is mostly controlled by  $K_{\text{max}}$  rather than  $\Delta K$ . The relative dependencies can be quantified by expressing the data in terms of a modified Paris power-law relation to include the effect of both  $\Delta K$  and  $K_{\text{max}}$ :

$$da/dN = C (\Delta K)^m (K_{\max})^p, \quad (1)$$

where  $C$  is a scaling constant (generally relatively independent of  $K_{\max}$ ,  $\Delta K$  and  $R$ ), and  $m$  and  $p$  are experimentally determined exponents. A regression fit to data in Fig. 5 yields  $m \sim 1.9$ , and  $p \sim 36$ , highlighting the marked dependence on  $K_{\max}$ . For results obtained at a given load ratio, Eq. (1) can be rewritten, using  $K_{\max} = \Delta K/(1 - R)$ , to give the more familiar form of the Paris equation:

$$da/dN = C'(\Delta K)^n, \quad (2)$$

where  $n = m + p$  and  $C' = C/(1 - R)^m$ . Values of the exponents  $n$ ,  $m$  and  $p$  are listed in Table 1 for a range of material systems. It is apparent that the exponent  $n$  in ceramics is characteristically much higher than the values of  $n \sim 2-4$  typically reported for metals (in the mid-range of growth rates) (15). However, in ceramics this results from a marked dependence on  $K_{\max}$ , i.e.,  $p \gg m$  whereas in metals,  $p \ll m$ .

The high growth-rate exponents, and in particular the marked  $K_{\max}$  dependence of growth rates, in ceramics results from a crack-advance mechanism identical to that under static loading; the much smaller dependence on  $\Delta K$  follows from the cyclic suppression of crack-tip shielding in the wake (6-9,16,17). Specifically, in grain-bridging ceramics such as  $Al_2O_3$ ,  $Si_3N_4$  and the present ABC-SiC ceramic, the degradation in shielding is dominated by progressive wear of the frictional grain bridges, i.e., of material in the grain boundaries between the sliding grains, during the opening and closing of the crack. This rapidly reduces the bridging tractions between the interlocking grains, thereby increasing the *near-tip* driving force for crack extension. Similar mechanisms have been reported in ceramic composites toughened by the bridging of partially bonded whiskers or fibers (9). Conversely, untoughened ceramics such as the commercial Hexoloy SA material are essentially immune to cyclic fatigue because transgranular crack morphology precludes the formation of any such shielding zones in the crack wake; these materials merely fail catastrophically when  $K_{\max} \rightarrow K_c$ .

Finally, since the mechanisms of static and cyclic fatigue in most ceramics at low homologous temperatures appear to be identical, to the first approximation, the maximum stress intensity at the fatigue threshold,  $K_{\max,TH}$ , should be approximately the same as the crack-initiation toughness,  $K_i$ , on the R-curve; experimental data for many ceramic systems (6,13,16-20) indeed confirm this notion.

TABLE 1 – Power-law exponents in fatigue-crack growth relationships at 25°C

Material	Total Exponent $n$	$\Delta K$ Exponent $m$	$K_{\max}$ Exponent $p$	Ref.
<i>Metals:</i>				
Ni-base superalloy	3.4	3.0	0.4	(15)
<i>Intermetallics</i>				
( $\gamma+\alpha_2$ )-TiAl	15.9	10.3	5.6	(32)
TiNb/ $\gamma$ -TiAl	12.4	6.3	6.1	(28)
Nb $_7$ /MoSi $_2$	20.7	7.5	13.2	(38)
<i>Ceramics</i>				
$Si_3N_4$	30.3	1.3	29.0	(20)
ABC-SiC	37.9	1.9	36.0	(13)
$Al_2O_3$	31.6	9.8	21.8	(19)
SiC $_w$ /Al $_2O_3$	15.0	4.8	10.2	(18)



**Behavior at elevated temperatures.** R-curve toughening is also evident in ABC-SiC at elevated temperatures (Fig. 6a). Both crack-initiation and steady-state toughness values are similar at ambient and 1200°C; the maximum toughness at 1200°C is some 11% higher, although the crack extends over larger dimensions (~2 mm) before reaching steady state. Such behavior can be attributed to softening of the largely amorphous grain-boundary phase, which reduces the magnitude of the bridging tractions but extends the length of the bridging zone. In fact, crack bridging by the glassy-phase ligaments can be observed to span the crack faces several millimeters behind the crack tip at the higher temperature (Fig. 6c), in contrast to the frictional interlocking of grains at ambient temperatures (Fig. 6d).

Mechanisms of fatigue-crack growth in ceramics at elevated temperatures are considerably more complex. Cyclic growth rates in ABC-SiC are nearly an order of magnitude faster at 1200°C than at 25°C, with the threshold  $\Delta K_{TH}$  value reduced from ~ 6.5 to ~4 MPa $\sqrt{m}$  (Fig. 6b); in addition, growth rates exhibit a lower dependence on  $\Delta K$  at the high temperature, similar to recent results on hot-pressed Si<sub>3</sub>N<sub>4</sub> (21). The acceleration of growth rates at elevated temperatures is likely due to enhanced creep deformation associated with the softening and cavitation of the glassy phase at grain boundaries, and to the reduced potency of the grain and viscous-phase bridging mechanisms under cyclic loading conditions at high temperatures.

Because of predominance of several competing mechanisms, namely intrinsic creep and perhaps fatigue damage, which promote crack growth, and grain and viscous-phase bridging, which act to oppose it, it is difficult to ascertain *a priori* whether cyclic fatigue or static creep crack growth is the more damaging at high homologous temperatures. It is clear that at ambient temperatures, cracks in toughened ceramics propagate much faster (at a given applied driving force) under cyclic compared to monotonic loads due to a cyclic suppression of the toughening; however, there is no consensus in the limited results that exist for high temperatures. For example, two separate studies on hot-pressed Si<sub>3</sub>N<sub>4</sub> report that cyclic crack-growth rates are faster (21) or slower (22) than corresponding growth rates measured under static loading. Such results are most likely the result of the fact that the prominent mechanisms, namely *intrinsic* creep/fatigue damage ahead of the crack tip via cavitation and grain-boundary sliding and *extrinsic* shielding from grain and viscous-film bridging, all depend upon the deformation and fracture properties of the amorphous grain-boundary phase; since this phase will be viscous at the higher temperatures, the relative potency of the various mechanisms will depend critically on the temperature and strain rate, as well as composition and environment. Thus, small differences in temperature, cyclic frequency, composition and environment may be expected to lead to large differences in behavior at elevated temperatures.

#### INTERMETALLIC MATERIALS

In general terms, fatigue-crack growth in metallic materials occurs by a largely  $\Delta K$ -controlled intrinsic damage mechanism (unique to cyclic loading) which advances the crack tip and is opposed by  $K_{max}$ -limited crack closure (wedge shielding) mechanisms in the wake. Conversely, crack growth in ceramic materials occurs by a  $K_{max}$ -controlled crack-advance mechanism (identical to static loading) and is opposed by  $\Delta K$ -limited wake shielding mechanisms that degrade under cyclic loads. Most intermetallic materials lie between these two extremes. For example, molybdenum disilicide behaves essentially as a ceramic, whereas titanium aluminide alloys display part metallic, part ceramic characteristics. Below such behavior is examined below for ductile-phase toughened  $\gamma$ -TiAl alloys.

### Titanium Aluminide Composites

**Behavior at Ambient Temperatures.**  $\gamma$ -TiAl based intermetallic alloys are currently of interest as low-density alternatives to conventional titanium alloys for use in gas-turbine engines; however, due to their brittle nature at ambient temperatures, much effort has been aimed at improving their tensile ductility and fracture toughness. Both composite reinforcement and alloying techniques have been used with considerable success to toughen  $\gamma$ -TiAl, which has an intrinsic toughness of less than 10 MPa $\sqrt{m}$  (23-28). One composite approach involves ductile-phase toughening (29) through the addition of a small amount of ductile metallic phases, e.g., Nb, TiNb or Ti-6Al-4V, into the microstructure. Depending upon how the crack interacts with this phase, which is a strong function of its morphology and interfacial bonding with the matrix, a variety of toughening mechanisms can ensue. Prominent among these are mechanisms which can increase the crack-initiation toughness, such as crack arrest, blunting and delamination at the interface, crack trapping by a particulate reinforcement, or crack renucleation across the ductile phase by a laminate reinforcement, and mechanisms of crack-growth (R-curve) toughening, such as extrinsic crack bridging by the uncracked ductile phase (Fig. 7).

A substantial improvement in fracture resistance of  $\gamma$ -TiAl can be achieved through reinforcement with ductile particles at room temperature (23,28). As shown in Fig. 8a, adding ~20 vol.% of  $\beta$ -TiNb particles to TiAl increases crack-initiation toughness to ~18 MPa $\sqrt{m}$ , more than twice that of pure  $\gamma$ -TiAl (~8 MPa $\sqrt{m}$ ); this can be attributed to crack trapping by TiNb particles and crack renucleation effects. The fracture resistance further increases with crack extension due to crack bridging by unbroken ductile TiNb ligaments in the crack wake (Fig. 8c). Indeed, these bridging zones under monotonic loading can be as large as ~3-6 mm (28), such that the results in Fig. 8a are undoubtedly influenced by large-scale bridging effects. The degree of toughening increases with volume fraction of reinforcements, but is independent of particle orientation. Similar toughening can be achieved through the addition of Nb particles; however, the TiNb reinforcements result in a larger toughness due to their much higher strength (yield stress for TiNb ~ 430 MPa compared to ~ 140 MPa for Nb).

Despite their effective role under monotonic loading, under cyclic loads, TiNb and Nb reinforcements result in only modest increases in the fatigue-crack growth resistance of  $\gamma$ -TiAl (Fig. 8b); moreover, this is achieved *only* for the C-L (face) orientation where faces of pan-cake shaped particles are oriented normal to the crack plane (28). In fact, for the C-R (edge) orientation where particle edges are oriented perpendicular to the crack plane, the incorporation of the ductile particles actually *degrades* the fatigue-crack growth properties relative to monolithic  $\gamma$ -TiAl. Such behavior in TiNb/TiAl is primarily due to the premature fatigue failure of ductile ligaments which restricts the development of a bridging zone and resultant shielding at the crack tip (Fig. 8d). In the face orientation, small shielding contributions from crack branching, matrix cracking and coplanar bridging within ~100-200  $\mu$ m behind the crack tip do provide a moderate increase in fatigue resistance, although these dimensions are far below the bridging-length scales observed during monotonic loading. The Nb-particulate reinforced TiAl alloys does show somewhat better fatigue-crack growth resistance (Fig. 8b). This is because the Nb particles are more weakly bonded to the matrix (the reaction layer consists of the brittle  $\sigma$  phase) compared to the TiNb particles (which has a strong reaction layer consisting of ductile  $\alpha_2$ +B2 phases). The resulting delamination at the Nb particle interface acts to delay the fatigue failure of the Nb ligaments such that they are more effective in preserving the shielding from crack bridging under cyclic loads.

Thus, similar to ceramic materials, cyclic loading acts progressively to degrade the toughening associated with wake shielding, in this case through the premature fatigue failure of the ductile bridging ligaments. However, unlike most ceramics, there may be an intrinsic mechanism of fatigue-crack advance in many intermetallics. Some insight can be achieved by examining the

separate dependencies of the growth rates on  $\Delta K$  and  $K_{\max}$ . In Fig. 9, fatigue-crack growth rates in the 20 vol.% TiNb/ $\gamma$ -TiAl alloy are shown at load ratios of  $R = 0.1, 0.5$  and  $0.7$  as a function of  $\Delta K$  and  $K_{\max}$ . As noted previously, increasing  $R$  accelerates crack-growth rates for a given  $\Delta K$  and lowers the fatigue threshold. Measured crack-closure levels are quite substantial at  $R < 0.4$  (closure stress intensities,  $K_c/K_{\min}$ , are  $\sim 0.4$ ), suggesting that shielding is important at the lower load ratios (28); however, marked differences in behavior between  $R = 0.5$  and  $0.7$  imply that other factors are relevant. What is apparent is that the variation in growth rates with load ratio is not normalized by  $K_{\max}$ , as was the case for ceramics (Fig. 5b), implying that cyclic crack growth in TiNb/TiAl composites is not governed solely by shielding mechanisms. This is also clear from examination of the respective dependencies on  $\Delta K$  and  $K_{\max}$  (Table 1); regression fits to the crack-growth data in Fig. 9 yield similar values for the  $\Delta K$  ( $m \sim 6.3$ ) and  $K_{\max}$  ( $p \sim 6.1$ ) exponents, implying a role of intrinsic fatigue damage in the composite. Such mechanisms of microstructural fatigue damage and cyclic crack advance are not understood in titanium aluminide intermetallics, but presumably are related to repeated blunting and sharpening of the crack in the TiAl and TiNb constituent phases, akin to behavior in ductile metals. In addition, static cleavage fracture modes are prevalent in the TiAl regions at higher growth rates, particularly at  $K_{\max}$  levels approaching  $K_c$  of the  $\gamma$ -TiAl matrix.

**Behavior at Elevated Temperatures.** Ductile TiNb particles also enhance the fracture resistance of  $\gamma$ -TiAl composites at elevated temperatures, specifically at  $650$  and  $800^\circ\text{C}$  (30), although the measured toughness is somewhat lower at  $650^\circ\text{C}$  (Fig. 10a). Crack bridging is still prominent during monotonic loading at high temperatures, although the tractions imposed in the crack wake are lower due to a reduced particle strength at the higher temperatures (30). However, this decrease in the efficiency of bridging is offset by an increase in intrinsic ductility and toughness of the TiAl matrix, especially above the ductile/brittle transition temperature for the  $\gamma$ -phase ( $\sim 700^\circ\text{C}$ ) (24); such competing effects account for the lower toughness of the composite at  $650^\circ\text{C}$ . However, ductile-phase toughening with a particulate phase such as TiNb or Nb may be severely compromised after prolonged exposure to elevated temperatures due to the poor oxidation resistance of the Nb-bearing phases. Protective coatings are thus essential to minimize environmental degradation if these materials are ever to find structural use.

At elevated temperatures, fatigue-crack growth is observed in the composite at  $\Delta K$  levels between  $\sim 4$ - $10$  MPa $\sqrt{\text{m}}$  (Fig. 10b), well below that needed to initiate crack growth under monotonic loading (where  $K_i \sim 12$ - $18$  MPa $\sqrt{\text{m}}$ ) (30). Although growth rates are slightly faster at  $650^\circ\text{C}$  than at  $25$  and  $800^\circ\text{C}$ , the dependency on applied  $\Delta K$  remains high at all temperatures ( $n \sim 7$ - $10$ ). Similar to behavior at  $25^\circ\text{C}$ , the TiNb particles fail prematurely by transgranular shear in fatigue to leave virtually no bridging zone (Fig. 10d); such behavior is quite distinct from the creation of an extensive zone of uncracked TiNb ligaments under monotonic loading, which ultimately fail by microvoid coalescence (Fig. 10c).

As with behavior at ambient temperatures, a principal factor influencing fatigue-crack growth is again the cyclic-loading induced suppression of ductile-ligament bridging. However, because of the reduced efficiency of such bridging at high temperatures (30), the premature failure of the bridges in fatigue does not significantly accelerate crack-growth rates in the composite relative to unreinforced TiAl. Indeed, at  $650^\circ\text{C}$ , cyclic crack-growth rates are essentially identical in the monolithic and composite alloys.

Thus in both ceramics and intermetallics, the extension of fatigue cracks is enhanced by the cycle-dependent degradation of bridging in the crack wake. There are significant differences though in the behavior of intermetallics. In TiNb/TiAl, fatigue-crack growth is seen at  $K$  levels far below the crack-initiation toughness,  $K_i$ , on the R-curve, specifically at a fatigue threshold of  $K_{\max,TH} \sim 0.25$ - $0.4 K_i$ . This implies that in addition to the *extrinsic* effects of limited shielding

under cyclic loading, there are *intrinsic* damage mechanisms uniquely associated with fatigue failure in intermetallics (Figs. 10c,d), as in metals. This is also evident in the differing dependencies of growth rates on  $\Delta K$  and  $K_{\max}$  in these material systems (Table 1). This is in sharp contrast to ceramics, where there are no intrinsic fatigue damage mechanisms at low homologous temperatures and crack advance occurs by identical mechanisms under monotonic and cyclic loads, such that  $K_{\max,TH} \sim K_I$ .

**DESIGN AND LIFE PREDICTION**

The marked sensitivity of fatigue-crack growth rates to the applied stress intensity in intermetallics and ceramics, both at elevated and especially ambient temperatures, presents unique challenges to damage-tolerant design and life-prediction methods for structural components fabricated from these materials. For safety-critical applications involving most metallic structures, such procedures generally rely on the integration of data relating crack-growth rates ( $da/dN$  or  $da/dt$ ) to the applied stress intensity ( $\Delta K$  or  $K_{\max}$ ) in order to estimate the time or number of cycles,  $N_f$ , to grow the largest undetectable initial flaw,  $a_i$ , to critical size  $a_c$ , viz:

$$N_f = \frac{2}{(n-2)C' (Q \Delta\sigma)^n \pi^{n/2}} [a_c^{(2-n)/2} - a_i^{(2-n)/2}] \tag{3}$$

where  $\Delta\sigma$  is the applied stress range,  $Q$  is the geometric factor;  $C'$  and  $n$  ( $\neq 2$ ) are the scaling constant and exponent in the crack-growth relationship in Eq. 2. For advanced materials such as intermetallics and ceramics, this approach may be difficult to implement in practice due to the large values of the exponent  $n$ ; since the projected life is proportional to the reciprocal of the applied stress raised to the power of  $n$ , a factor of two change in applied stress can lead to projections of the life of a ceramic component (where  $n$  can be as high as 20 or more) to vary by more than six orders of magnitude. Essentially, because of the high exponents, the life spent in crack propagation in advanced materials will be extremely limited or infinitely large, depending upon whether the initial stress intensity is above or below the fatigue threshold.

Accordingly, a more appropriate approach may be to design on the basis of a threshold below which fatigue failure cannot occur; this may involve a conventional fatigue-crack initiation threshold or fatigue limit determined from stress-life (S/N) data or, more conservatively, the  $\Delta K_{TH}$  or  $K_{\max,TH}$  thresholds for no crack growth. However, even these approaches may not be conservative due to uncertainties in the definition of such thresholds. This is particularly important in many advanced materials as their growth-rate and S/N curves are not sigmoidal and correspondingly show no evidence of a threshold (Fig. 11). Moreover, as with metallic materials (e.g., 31,32), there is now increasing evidence for small-crack effects in both ceramics and intermetallics, where cracks of a size comparable with the scale of microstructure, the extent of local inelasticity ahead of the crack tip, or with the extent of shielding in the wake of the tip, can propagate at applied stress intensities *below* the “long-crack”  $\Delta K_{TH}$  or  $K_{\max,TH}$  thresholds (e.g., 18). Clearly for flaw-sensitive materials such as ceramics and intermetallics to be safely used in fatigue-critical applications, the critical levels of damage necessary for the *onset* of fatigue failure must be defined; whether this involves an S/N fatigue limit, long- or small-crack thresholds, or more refined statistical analyses is as yet still unclear.

**CONCLUDING REMARKS**

Major progress has been made over the last ten to fifteen years in significantly improving the fracture resistance of low-ductility materials such as ceramics and intermetallics using the extrinsic shielding approach to toughening. This has included the design of microstructures which develop zones of inelasticity, microcracking or bridging (by grains, particulate or fibers) that surround the

crack. However, it is now evident that in most instances, cyclic loading can severely degrade such shielding; in fact, this provides the critical mechanism promoting fatigue-crack growth, even in materials such as ceramics which display no intrinsic mechanism of cyclic crack advance.

Between the various classes of materials, fatigue-crack growth rate data suggest that the general dependency of growth rates on stress intensity (i.e.,  $n$ ) increases, and the fatigue threshold decreases, with decreasing ductility (Fig. 13). Indeed, whereas  $\Delta K_{TH}$  thresholds in metals can be as small as  $0.1K_c$ , in the most brittle ceramics,  $\Delta K_{TH} \sim K_c$ . However, there is a certain commonality that can be deduced through a general consideration of which intrinsic and extrinsic mechanisms are active (e.g., Fig. 1) and their relative dependence on mean or alternating loads:

- In ductile metals (Fig. 3a), crack advance is promoted by an intrinsic mechanism ahead of the tip (unique to cyclic fatigue), for example, by alternating crack-tip blunting and resharpening. Since this is primarily controlled by the alternating plastic strain, the primary dependence is on  $\Delta K$ , although a smaller intrinsic  $K_{max}$  dependence may arise due to the occurrence of static fracture modes, particularly as  $K_{max}$  approaches  $K_c$ . Crack advance is impeded by extrinsic shielding behind the crack tip, which in metals is primarily associated with crack wedging mechanisms (crack closure). Since the degree of wedging depends critically on the relative size of the maximum crack-tip opening displacements, this leads to a much smaller dependency on  $K_{max}$ , i.e.,  $p \ll m$ .
- In brittle ceramics (Fig. 3b), crack advance is promoted by a mechanism ahead of the tip that is identical to that occurring under static loading, e.g., intergranular cracking. Since this is controlled by the maximum load, the primary dependence is on  $K_{max}$ . Crack advance is once again impeded by extrinsic shielding behind the crack tip, which in most ceramics and their composites is associated with crack bridging; however, as cyclic loading acts progressively to diminish the potency of such wake shielding, this leads to a much smaller dependency on  $\Delta K$ , i.e.,  $p \gg m$ .
- In intermetallics, fatigue properties are intermediate between the extremes of "metal-" and "ceramic-like" behavior, i.e.,  $p \sim m$ . In brittle intermetallics such as  $MoSi_2$ , where there is no intrinsic cycle-dependent crack advance mechanism,  $p > m$ . In more ductile materials, such as the  $(\gamma+\alpha_2)$  TiAl alloys, intrinsic fatigue damage mechanisms, similar to those in metals, clearly exist, i.e.,  $p < m$ . However, in most intermetallics, extrinsic ("ceramic-like") crack-bridging mechanisms in the wake are generally degraded under cyclic loads, although the fatigue resistance is often not compromised as they can be replaced by the development of ("metal-like") crack-closure mechanisms.

It should be noted that the existence of active wake-shielding mechanisms such as crack bridging or crack closure has other significant implications for fatigue and fracture behavior. Clearly, there will be a loss of similitude between cracks of varying size if considerations are based on the applied (or nominal) stress intensities. Accordingly, since small cracks will have more limited wakes, they are likely to experience a higher *local* driving force due to reduced shielding. This results in R-curve behavior under monotonic loading and the well known sub-threshold growth of small cracks in cyclic fatigue. In addition, since shielding can have little influence on crack initiation, it is to be expected that microstructures designed for optimal crack-growth resistance may be quite different to those designed for optimal resistance to crack initiation or small-crack growth.

Finally, the marked sensitivity of growth rates to the applied stress intensity in ceramics and intermetallics implies that projected lifetimes will be a very strong function of stress and crack size; this makes design and life prediction using damage-tolerant methodologies extremely difficult. Accordingly, design approaches based on the definition of a critical level of damage for the *onset* of fatigue cracking must be contemplated, involving either an S-N fatigue limit or crack-propagation threshold, although even these approaches may not be conservative due to the sub-

threshold extension of small cracks. Clearly, this is an area that mandates increased attention in the future if these materials are to find widespread structural use.

#### ACKNOWLEDGMENTS

This work was supported by the U.S. National Science Foundation under Grant No. DMR-9522134 (for high temperature studies on ceramics), the Office of Energy Research, Office Basic Energy Sciences, Materials Sciences Division of the U.S. Department of Energy under Contract No. DE-AC03-76SF00098 (for research on SiC), and the U.S. Air Force Office of Scientific Research under Grant Nos. F49620-93-1-0107 and 0289 (for studies on intermetallics). Our particular thanks are due to C. J. Gilbert for his work on SiC, and to Profs. G. R. Odette and L. C. DeJonghe for their collaboration and helpful discussion.

#### REFERENCES

- (1) Ritchie, R. O., *Mater. Sci. Eng. A*, Vol. A103, 1988, pp. 15-28.
- (2) Evans, A. G., *J. Am. Ceram. Soc.*, Vol. 73, 1990, pp. 187-206.
- (3) Liu, C. T., Stiegler, J. O., and Froese, F. H., "Metals Handbook," ASM Intl., Materials Park, OH, Vol. 2, p. 913, 1991.
- (4) Elber, W., *Eng. Fract. Mech.*, Vol. 2, 1970, pp. 37-45.
- (5) Suresh, S., and Ritchie, R. O., in "Fatigue Crack Growth Threshold Concepts". Edited by D.L. Davidson and S. Suresh, TMS-AIME, Warrendale, PA, pp. 227-261, 1984.
- (6) Ritchie, R. O., and Dauskardt, R. H., *J. Ceram. Soc. Japan*, Vol. 99, 1991, pp. 1047-1062.
- (7) Lathabai, S., Rödel, J., and Lawn, B., *J. Am. Ceram. Soc.*, Vol. 74, 1991, pp. 1340-1348.
- (8) Dauskardt, R. H., *Acta Metall. Mater.*, Vol. 41, 1993, pp. 2765-2781.
- (9) Rouby, D., and Reynaud, P., *Compos. Sci. Technol.*, Vol. 48, 1993, pp. 109-118.
- (10) Laird, C., and Smith, G. C., *Philos. Mag.*, Vol. 7, 1962, pp. 847-857.
- (11) Neumann, P., *Acta Metall.*, Vol. 17, 1969, pp. 1219-1225.
- (12) Cao, J. J., MoberlyChan, W. J., DeJonghe, L. C., Gilbert, C. J., and Ritchie, R. O., *J. Am. Ceram. Soc.*, Vol. 79, 1996, pp. 461-469.
- (13) Gilbert, C. J., Cao, J. J., MoberlyChan, W. J., DeJonghe, L. C., and Ritchie, R. O., *Acta Mater.*, Vol. 44, 1996, in press.
- (14) Srinivasan, M., in "Structural Ceramics," *Treatise on Materials Science and Technology*. Edited by J.B. Wachtman, Jr., Academic Press, New York, NY, Vol. 29, pp. 99-159, 1989.
- (15) VanStone, R. H., *Mater. Sci. Eng. A*, Vol. A103, 1988, pp. 49-61.
- (16) Kishimoto, H., *JSME Intl. J.*, Vol. 34, 1991, pp. 393-403.
- (17) Jacobs, D. S., and Chen, I.-W., *J. Am. Ceram. Soc.*, Vol. 78, 1995, pp. 513-520.
- (18) Dauskardt, R. H., James, M. R., Porter, J. R., and Ritchie, R. O., *J. Am. Ceram. Soc.*, Vol. 75, 1992, pp. 759-771.
- (19) Gilbert, C. J., Dauskardt, R. H., Steinbrech, R. W., Petrany, R. N., and Ritchie, R. O., *J. Mater. Sci.*, Vol. 30, 1995, pp. 643-654.
- (20) Gilbert, C. J., Dauskardt, R. H., and Ritchie, R. O., *J. Am. Ceram. Soc.*, Vol. 78, 1995, pp. 2291-2300.
- (21) Ramamurty, U., Hansson, T., and Suresh, S., *J. Am. Ceram. Soc.*, Vol. 77, 1994, pp. 2985-2999.
- (22) Liu, S.-Y., Chen, I.-W., and Tien, T.-Y., *J. Am. Ceram. Soc.*, Vol. 77, 1994, pp. 137-142.
- (23) Elliott, C. K., Odette, G. R., Lucas, G. E., and Shekherd, J. W., in "High-Temperature/High-Performance Composites." Edited by F.D Lemkey, A.G. Evans, S.G. Fishman, and J.R. Strife, Materials Research Society, Pittsburgh, PA, Vol. 120, pp. 95-101, 1988.
- (24) Lipsitt, H. A., Schectman, D., and Schafrik, R. E., *Metall. Trans. A*, Vol. 6A, 1975, pp. 1991-1996.
- (25) Kim, Y. W., and Dimiduk, D. M., *J. Metals*, Vol. 43, No.8, 1991, pp. 40-47.

- (26) Dève, H. E., Evans, A. G., and Shih, D. S., *Acta Metall. Mater.*, Vol. 40, 1992, pp. 1259-1265.
- (27) Chan, K. S. and Kim, Y.-W., *Metall. Trans. A*, Vol. 23A, 1992, 1663-1677.
- (28) Venkateswara Rao, K. T., Odette, G. R., and Ritchie, R. O., *Acta Metall. Mater.*, Vol. 42, 1994, pp. 893-911.
- (29) Ashby, M. F., Blunt, F. J., and Bannister, M., *Acta Metall. Mater.*, Vol. 37, 1989, pp. 1847-1857.
- (30) Venkateswara Rao, K. T., and Ritchie, R. O., in "Fatigue and Fracture of Ordered Intermetallics and Compounds II." Edited by W.O. Soboyejo, T.S. Srivatsan, and R.O. Ritchie, TMS, Warrendale, PA, pp. 327-338, 1995.
- (31) Ritchie, R. O., and Lankford, J., eds., "Small Fatigue Cracks", TMS-AIME, Warrendale, PA, 1986.
- (32) Miller, K. J. and de los Rios, E. R., eds., "Short Fatigue Cracks", Mech. Eng. Publ. Ltd., London, U.K., 1992.

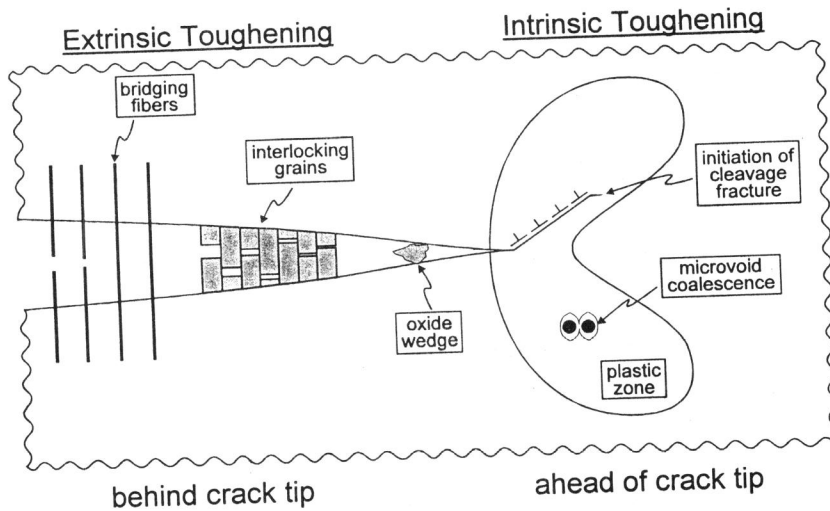


Figure 1 Schematic illustration of the mechanisms involved in crack growth, specifically, *intrinsic* mechanisms, such as transgranular cleavage and microvoid coalescence, are active in the process zone *ahead* of the crack tip and act to promote cracking; *extrinsic* mechanisms, such as fiber bridging, grain bridging and oxide wedging, are active in the wake *behind* the crack tip and act to inhibit cracking.

EXTRINSIC TOUGHENING MECHANISMS

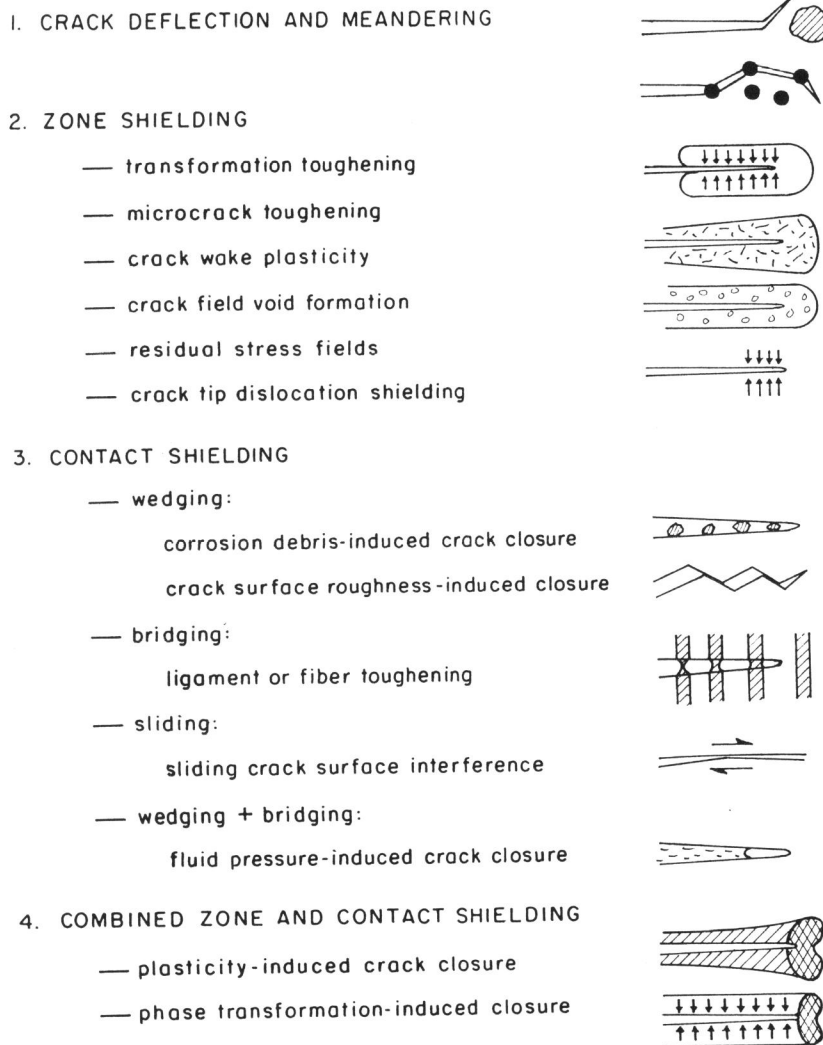


Figure 2 Schematic representation of the classes and micromechanisms of extrinsic toughening by crack-tip shielding (1).



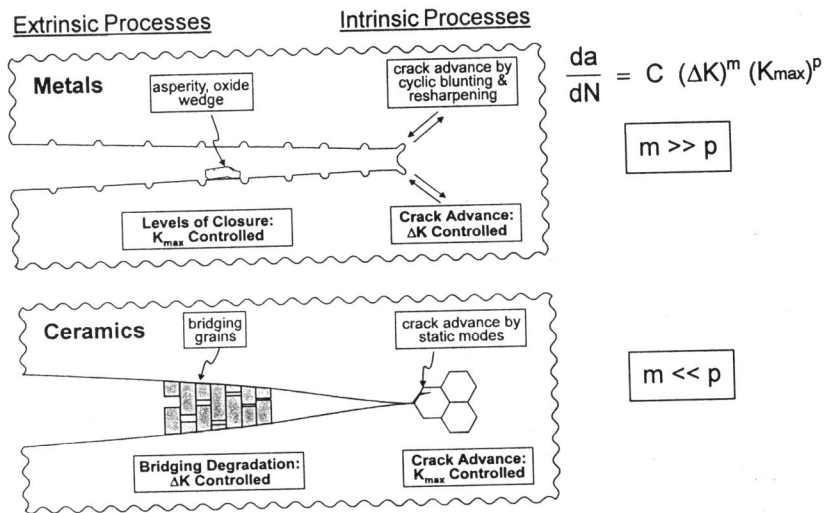


Figure 3 Schematic illustrations of the intrinsic and extrinsic mechanisms involved in cyclic fatigue-crack growth in (a) metals and (b) ceramics, showing the relative dependencies of growth rates,  $da/dN$ , on the alternating,  $\Delta K$ , and maximum,  $K_{max}$ , stress intensities.

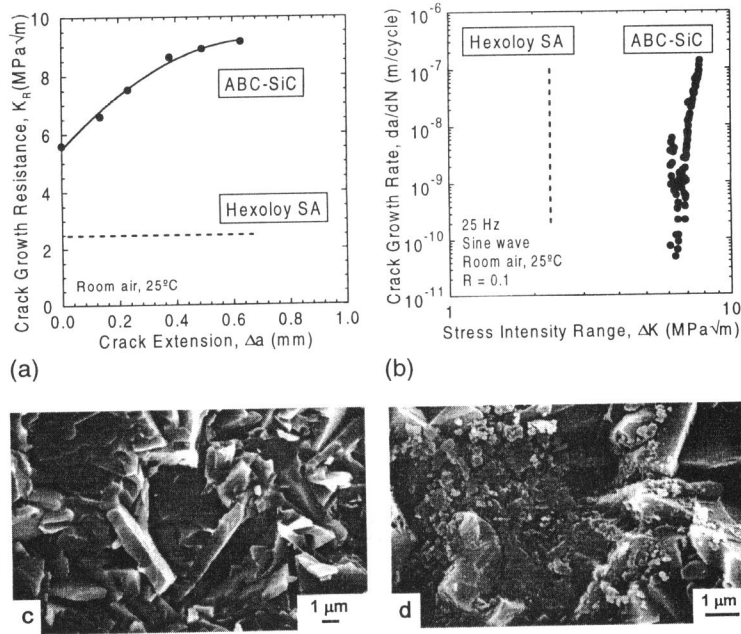


Figure 4 (a) Resistance curve and (b) fatigue-crack growth behavior in an *in situ* toughened ABC-SiC in room temperature air ( $R = 0.1$ , 25 Hz), compared to corresponding behavior in a commercial SiC (Hexoloy SA) that shows no apparent R-curve or susceptibility to fatigue. (c) Clean and faceted intergranular failures observed during monotonic loading, and (d) wear debris on the fracture surface from repetitive grain sliding under cyclic loading (13).

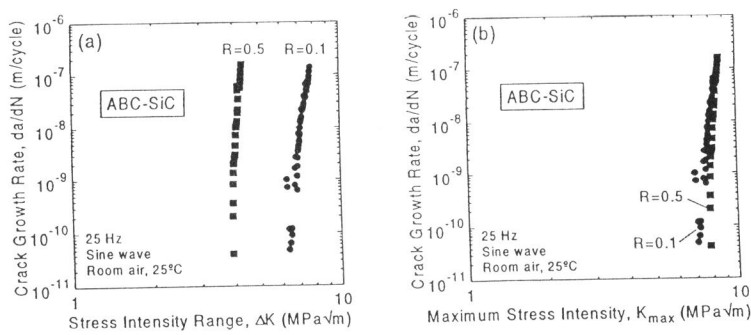


Figure 5 Variation in fatigue-crack propagation rates in ABC-SiC at different load ratios, plotted as a function of (a) the applied stress-intensity range,  $\Delta K$ , and (b) the maximum stress intensity,  $K_{max}$ . Note that the data are normalized when characterized in terms of  $K_{max}$ , suggesting that the cyclic crack-advance mechanism is similar to that for static fatigue (13).

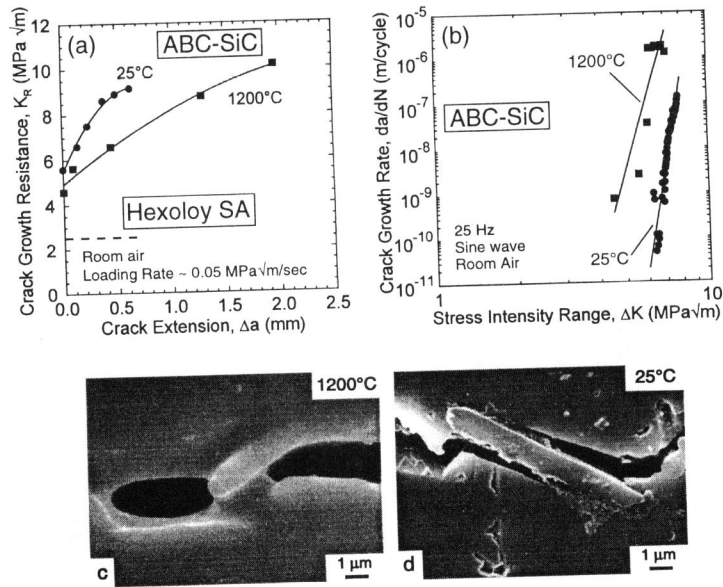


Figure 6 (a) R curves and (b) fatigue-crack propagation behavior in ABC SiC at 25° and 1200°C in air (at  $R = 0.1$  with 25 Hz frequency). Note that R-curve toughening at 1200°C is associated with (c) bridging from viscous films present at grain boundaries, whereas at ambient temperatures, it involves (d) frictional grain bridging.

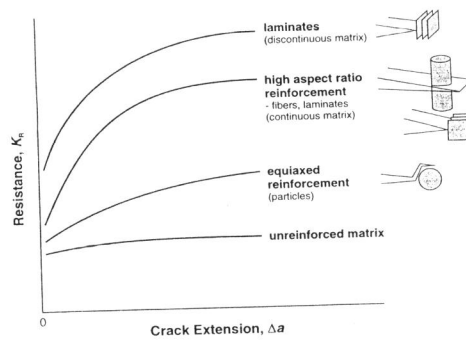


Figure 7 Schematic illustration of R-curve behavior for brittle-matrix composites reinforced with particulate, fibers or laminates as a ductile phase. Mechanisms that increase the crack-initiation toughness (where  $\Delta a \rightarrow 0$ ) include crack trapping by particles and crack renucleation by laminates; corresponding mechanisms that increase the crack-growth toughness include crack bridging by intact ductile phases or uncracked ligaments.

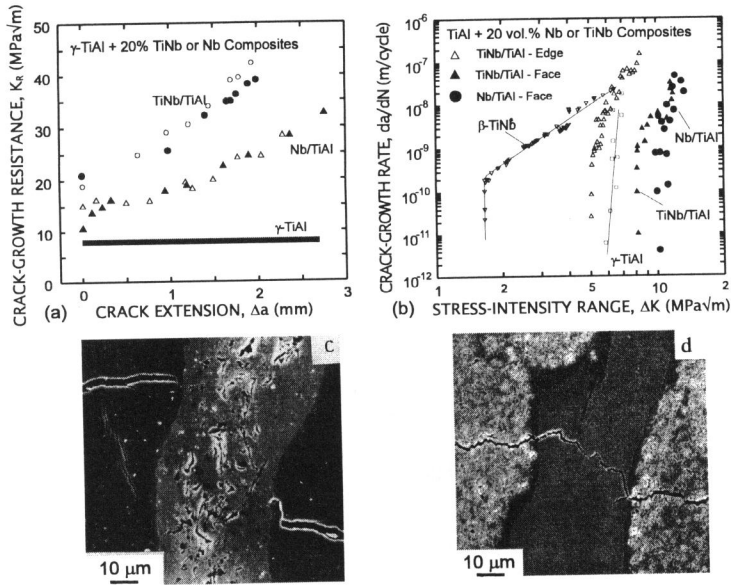


Figure 8 (a) Fracture toughness and (b) fatigue-crack growth behavior in a 20 vol.% TiNb-reinforced  $\gamma$ -TiAl composite at room temperature (at  $R = 0.1$  with 25 Hz frequency), in the edge (C-R) and face (C-L) orientations; results are compared to data in pure  $\gamma$ -TiAl,  $\beta$ -TiNb and a Nb-particulate reinforced  $\gamma$ -TiAl composite. (c) Extensive crack bridging by the uncracked ductile phase under monotonic loading is severely degraded under cyclic loading due to (d) premature fatigue failure of the ductile ligaments (28).

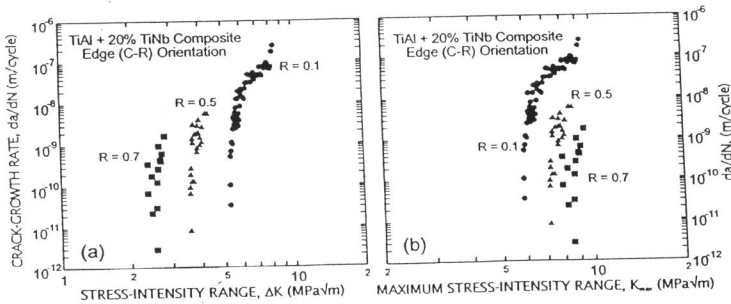


Figure 9 Fatigue-crack propagation rates in the TiNb/ $\gamma$ -TiAl composite at various load ratios, characterized in terms of (a) the applied stress-intensity range,  $\Delta K$ , and (b) the maximum stress intensity,  $K_{max}$ . Note that, unlike the SiC ceramic in Fig. 5,  $K_{max}$  does not normalize the growth-rate data.

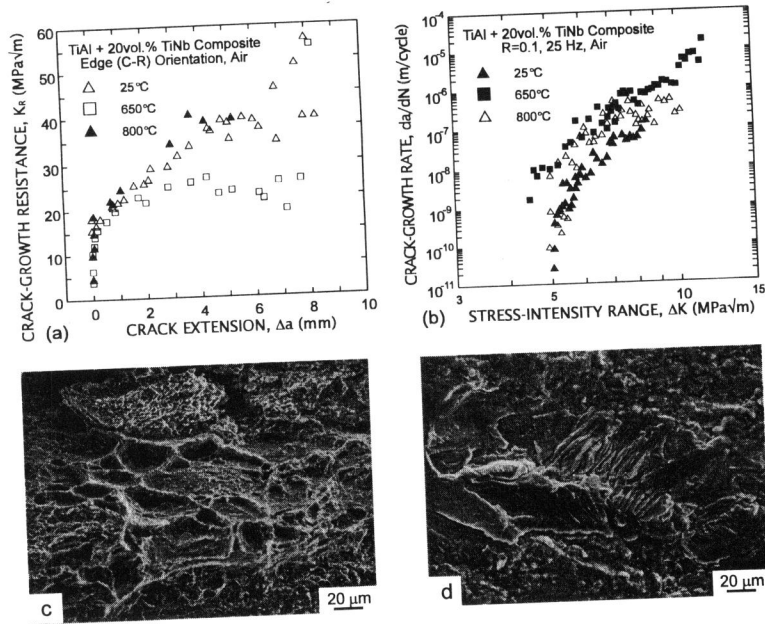


Figure 10 (a) Fracture toughness and (b) fatigue-crack growth behavior (at  $R = 0.1$  with 25 Hz frequency), in the TiNb/ $\gamma$ -TiAl composite (edge (C-R) orientation) at various temperatures; corresponding fracture surfaces at 800°C, under (c) monotonic and (d) cyclic loading, are also shown. Note the clearly distinct (microvoid coalescence vs. transgranular shear) failure modes in the TiNb under monotonic and cyclic loading (30).

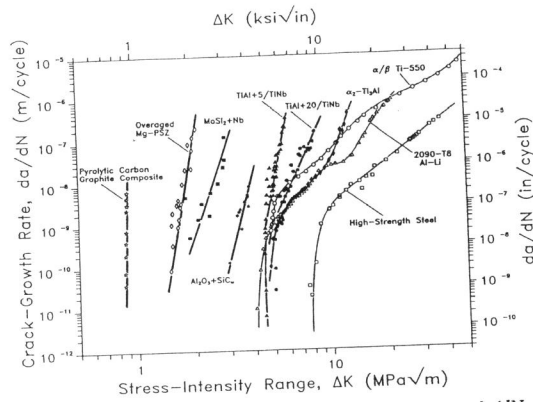


Figure 11 A compendium of cyclic fatigue-crack propagation data,  $da/dN$ , as a function of the applied stress-intensity range,  $\Delta K$ , in metallic alloys, monolithic and composite intermetallics, and monolithic and composite ceramics.